J IRAN CHEM SOC (2013) 10:799–805
DOI 10.1007/s13738-012-0215-z

ORIGINAL PAPER

Effect of silver nanoparticles concentration on the metal enhancement and quenching of ciprofloxacin fluorescence intensity

Alireza Farokhcheh · Naader Alizadeh

Received: 11 September 2012 / Accepted: 27 December 2012 / Published online: 23 January 2013

Abstract Concentration effect of silver nanoparticles (AgNPs) on the photophysical properties of ciprofloxacin (Cip) have been investigated using optical absorption and fluorescence techniques. When performed AgNPs solution was added to the Cip solution, metal-enhanced fluorescence intensity and a blue-shift of 20 nm in the maximum emission spectra of Cip has been observed. The enhanced intensity of this system is strongly dependent on the AgNPs concentration and largest at the 6.0×10^{-6} mol L^{-1}. With increase of AgNPs concentration, quenching of fluorescence is observed. Stern–Volmer quenching constants have been calculated at four temperatures. The results show the quenching constants are directly correlated with temperature. It indicates the quenching mechanism is the dynamic quenching in nature rather than static quenching. From which we determined the activation energy for the quenching of Cip-AgNPs to be about 31.1 kJ mol^{-1}. In addition, in the presence of optimum AgNPs concentration, a sensitive fluorimetric method for the determination of ciprofloxacin at the range 5.0×10^{-7}–3.0×10^{-5} mol L^{-1} and the detection limit of 2×10^{-8} mol L^{-1} in solution is proposed.

Keywords Silver nanoparticles · Ciprofloxacin · Metal-enhanced fluorescence · Quenching

A. Farokhcheh · N. Alizadeh (✉)
Department of Chemistry, Faculty of Science, Tarbiat Modares University, P.O. ox 14115-175, Tehran, Iran
e-mail: alizaden@modares.ac.ir

Introduction

Metal nanoparticles have been investigated intensively in recent years because of their size-dependent electronic and optical properties and the possibility of arranging them in micro and nano-assemblies [1]. In particular, a lot of effort has been devoted to the synthesis and characterization of stable dispersions of nanoparticles made of silver, gold, and other noble metals [2, 3]. Due to surface plasmon excitation, nanoparticles of silver, gold, and copper may exhibit sharp electronic absorption bands in the visible region spectrum [3]. Among them, silver nanoparticles have been widely studied due to their useful optical, electrical, and catalytic properties [4–9]. With the progress of nanotechnologies and the spectral theories, the luminescence properties of metal nanoparticles have been studied [10–13]. Resonant energy transfer systems consisting of organic dye molecules and noble metal nanoparticles have recently gained considerable interest in biophotonics as well as in materials science [14]. Interaction of a dye with the medium at the molecular level is reflected in its visible and fluorescence spectra [15]. This interaction between the fluorophor-metal nanoparticle or fluorophor-quantum dot is a lot of attention because of important in design novel with materials electrical, optical, lithographic, sensing, and photochemical properties [16, 17]. Fluorescence detection is a central technology of biosciences. While fluorescence can be a very sensitive technique, the detection of a fluorophore is usually limited by its quantum yield, autofluorescence of the sample and the photostability of the fluorophores. In this regard, one important strategy to achieve fluorescence enhancement is to utilize metallic nanoparticles, which are known to drastically alter the emission of vicinal fluorophores. Enhancement of dye fluorescence by gold and silver

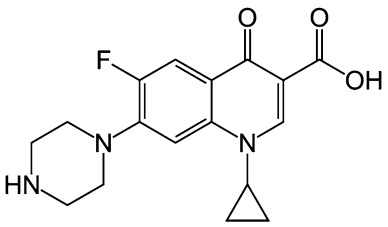

Scheme 1 Chemical structure of ciprofloxacin

nanoparticles has already been observed experimentally [18–21], including the first use and introduction of the term "metal-enhanced fluorescence" (MEF).

Improvements in the analytical utility of MEF-based sensors will require recognition of other reaction that may be compete with the desired reaction, such as quenching process. One type of quenching is due to collisions between quenching agents and fluorophores, and is called collisional or dynamic quenching. The dynamic quenching provides a non-radiative route for loss of the excited state energy. A second type of quenching, sometimes confused with dynamic quenching, is static quenching, in which the quencher forms a non-fluorescent complex with the quenching agent. Toward to the better understanding these processes, we have sought to study fluorophor-metal nanoparticle interaction, with enhance and quenching effects.

Ciprofloxacin (Cip) belongs to the family of fluoroquinolone antibacterial agents that also include enoxacin, norfloxacin, ofloxacin and some other molecules (Scheme 1). These fluoroquinolone antibacterial agents are synthetic derivatives of 6-fluoro-4-oxo-quinoline-3-carboxylic acid. They are fluorinated at position 6 and mostly bear a piperazinyl moiety at position 7. Cip is one of the most potent quinolone derivatives in clinical use with a very broad spectrum of antibacterial activity and is often used as an antibacterial agent [22–25].

The present work is a continuation of our earlier studies on the investigation of different effect on the fluorescence intensity of various systems [26–30]. In this study, optical absorption and fluorescence emission techniques have been employed to investigate the effect of silver nanoparticles concentration on the enhancement and quenching of fluorescence intensity of Cip (Scheme 1).

Experimental section

Reagents and procedure

All the chemicals and reagents analytical grade were from Merck (Darmstadt, Germany) and doubly deionized water was used throughout. Ciprofloxacin hydrochloride monohydrate powder was obtained from Amin Co., Iran. Stock standard solution of 10^{-4} mol L^{-1} was prepared by dissolving accurately measured amounts of Cip in double distillated water. The pH values in optimization stage were adjusted by sodium acetate/acetic acid buffer addition. The silver nanoparticles (AgNPs) in the presence of a cationic surfactant, cetyltrimethylammonium bromide (CTAB) were synthesized by following the literature [31]. In brief, 25 mL of silver nitrate solution (6.0×10^{-4} mol L^{-1}) is mixed with CTAB (2.0×10^{-4} mol L^{-1}) and then adding the mixed Ag^{+}-CTAB drop wise to 25 mL of sodium borohydride solution (1.2×10^{-3} mol L^{-1}) with vigorous stirring. It was repeated for different volume of sodium borohydride (4, 8, and 10 mL) at constant volume of silver nitrate solution (25 mL). Both the solutions were chilled to ice temperature. The reaction is performed in an ice-cooled water bath to reduce the reaction rate, and ionic surfactants are used as stabilizers in order to obtain stable silver colloids.

Apparatus

Optical absorption spectra were recorded using a (Scinco model 2100) UV-visible spectrophotometer with quartz cell of 1 cm path length. The fluorescence spectra were recorded by a Perkin–Elmer model LS 50B spectrofluorimeter equipped with a thermostated cell compartment, at all temperatures used, the accuracy of temperature measurement was ±0.1 °C. Fluorescence data were obtained by using the slit-width of the excitation and the emission of the spectrofluorometer at 10 nm and the excitation wavelength was 335 nm. Powder X-ray diffraction (XRD) patterns were measured using Cu-Kα radiation ($\lambda = 1.5406$ Å) on a Philips. Scanning electron microscopy (SEM) was done on a Philips XL-30 instrument. Infrared spectra were recorded at 4 cm^{-1} resolution with a Nicolet 100 Fourier transform infrared (FT-IR) spectrometer. The results of the enhancing reactions between the AgNPs and Cip were analyzed according to the Stern–Volmer and Benesi–Hildberant equation [32, 33].

Preparation of sample tablet solutions

Ten tablets were weighed, finely powdered, and portions equivalent to 500 mg Cip were transferred into a 100 mL volumetric flask; 50 mL water was added, shaken thoroughly to dissolve, was brought to volume, mixed well and centrifuged; the supernatant was used to prepare solutions of 10^{-3} mol L^{-1} of Cip using water as the diluents. The working sample solution (10^{-3} mol L^{-1}) obtained by dilution of supernatant was used to set up the concentrations in the range of calibration studies and 6.0×10^{-6} mol L^{-1} AgNPs was added to each of sample.

Results and discussion

Spectral characteristics of AgNPs drug interaction

The UV-vis spectrum of the as-prepared AgNPs (5.0×10^{-5} mol L^{-1}) is shown in Fig. 1a. It exhibits a surface plasmon resonance band at 400 nm, which arise due to collective oscillations of the conduction electrons in the electromagnetic field of the incident light [34]. The observed plasmon band shows that the AgNPs are spherical in shape [35, 36]. In Fig. 1b, we show XRD patterns of the AgNPs. The obtained XRD spectrum of silver nanoparticles is matched with JCPDS Card No. 4-0783, which exhibits the characteristic peaks of the silver crystallites observed at $2\theta = 38.09°$ (111), 44.33° (200), and 64.49° (220). The position of the XRD peaks of the Ag nanoparticles matches with those from metallic Ag in the face-centered cubic phase. Thus, the XRD spectrum confirmed the crystalline structure of silver corresponds to the particles 35 nm diameter [37].

Figure 1c shows SEM image of AgNPs. Average size of the particles is 55 nm and nanoparticles are spherical in shape. Also, in the Fig. 1d, we show the FT-IR spectra of pure CTAB (solid line) and CTAB-capped AgNPs (dash line) in regions of 500–4,000 cm^{-1}. We can clearly observe the CH_2- and CH_3-stretching modes in 3,000–2,800 cm^{-1} [38], the CH_2 bending mode and the CH_3–(N^+) deformation mode in 1,500–1,450 cm^{-1}, and the CH_2 rocking mode in 735–710 cm^{-1} [38], which appears in spectra of aqueous and crystal CTAB. The spectra give unambiguous evidence of sorbed CTAB on AgNPs.

The spectrum of Cip in aqueous solution exhibits an absorbance maximum at 276, 324 and 335 nm (Fig. 2a) and does not interfere with the plasmonic absorption band of AgNPs located in the visible range of the spectrum. However, when Cip solution was added to the preformed AgNPs solution, a noticeable decrease in total absorbance and a slight blue-shift of 3 nm in the maximum absorbance of plasmonic band were measured (see Fig. 2a, curve c), which clearly indicated the interaction of drug and AgNPs. The spectral shift confirms the existence of drug-AgNPs interaction. The absorption maximum at 276 nm corresponds to the π–π^* transition of the fluorobenzene moiety, and other two correspond to n–π^* as well as

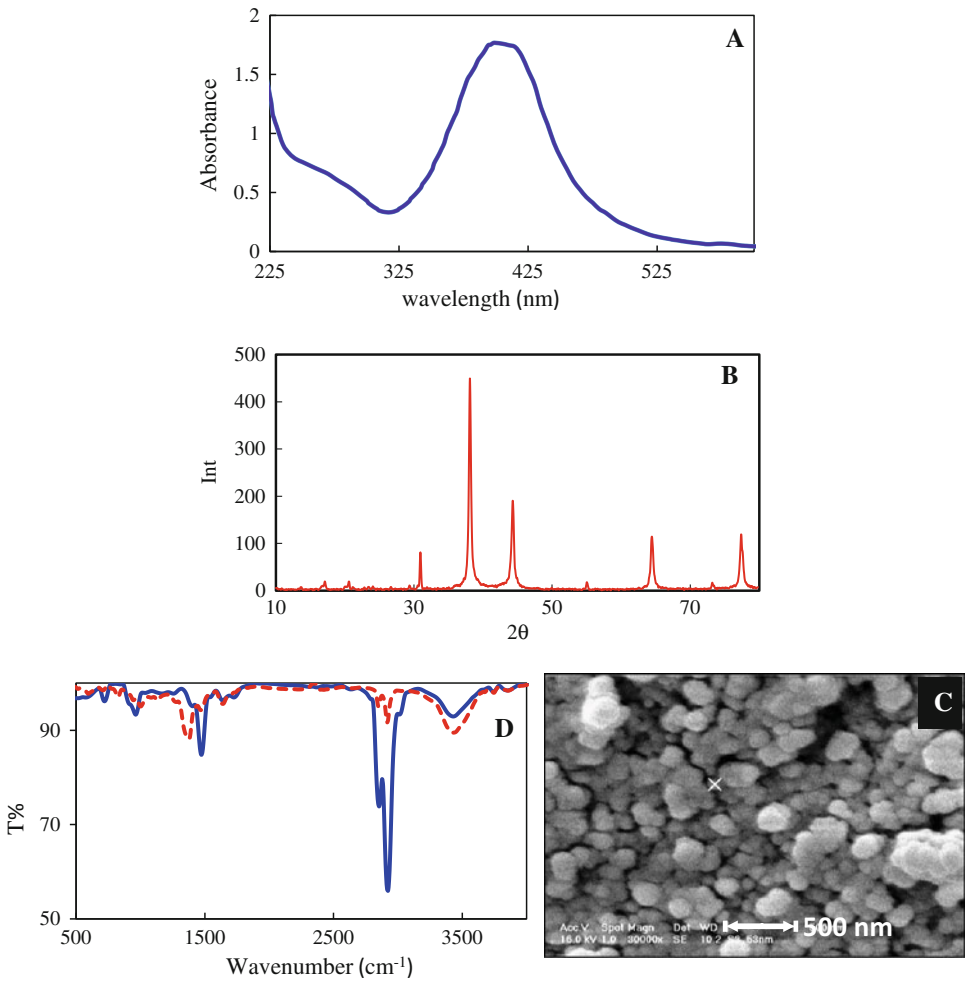

Fig. 1 Spectroscopic characterization of AgNPs; Absorption spectrum (**a**), X-ray diffractogram (**b**), SEM image of AgNPs (**c**), FT-IR spectrum of CTAB (*solid line*) and CTAB capped AgNPs (*broken line*) (**d**)

π–π*transitions of the quinolone ring [39] (Scheme 1). After adsorption, the peak at 276 nm is shifted to 270 nm and the other absorption peaks of Cip molecules at 324 and 335 nm also get shifted to longer wavelength (Fig. 2a, curve c). The UV–visible spectra of AgNPs were also recorded in different concentration of Cip in aqueous solution Fig. 2b.

The equilibrium for the formation of the complex between Cip and AgNPs can be given as shown below.

$$K_{as} = [\text{AgNPs} - \text{Cip}]/[\text{AgNPs}][\text{Cip}] \quad (1)$$

The Benesi–Hildebrand equation can be utilized to obtain

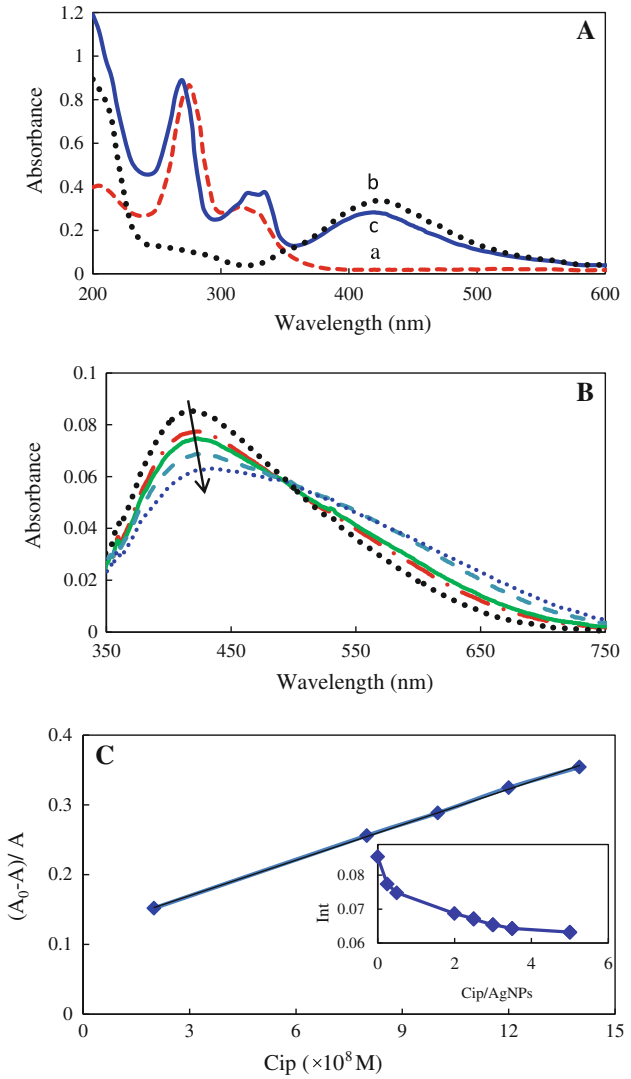

Fig. 2 **a** Absorption spectrum of *a* Cip 1.0×10^{-5} mol L^{-1}, *b* AgNPs 1.5×10^{-5} mol L^{-1}, *c* AgNPs 1.5×10^{-5} mol L^{-1} and Cip 1.0×10^{-5} mol L^{-1}; **b** absorption spectra of AgNPs (4.0×10^{-6} mol L^{-1}) in presence of (*top* to *bottom*) 0, 2.0×10^{-8}, 8.0×10^{-8}, 1.0×10^{-7}, and 2.0×10^{-7} mol L^{-1} of Cip (*arrow*, shows direction of change of the band) and **c** plot of $(A_0 - A)/A$, plasmonic absorbance of AgNPs versus [Cip]. Variation of plasmonic absorbance versus Cip/AgNPs mole ratio (*insert*)

K_{as} by using the changes in the absorption at plasmonic band of AgNPs (4.0×10^{-6} mol L^{-1}) at 400 nm. The association constant of $K_{as} = 1.70 \times 10^6$ L mol^{-1} was obtained from the plot of $(A_0 - A)/A$ versus [Cip]. A_0 and A are the observed absorbance of the solution in the absence and presence of drug at different concentrations (2.0×10^{-8}–20.0×10^{-8} mol L^{-1}), respectively. The high value of K_{as} observed in these experiments suggests a strong association between the AgNPs and Cip. The variation of plasmonic absorbance versus Cip/AgNp mole ratio was inserted in Fig. 2c.

Fluorescence spectra analysis

Enhancing and quenching of fluorescence is a technique to understand the interaction within the medium in view of the special role of surfaces of the nanoclusters in guiding and modifying physicochemical processes. In Fig. 3a, b fluorescence spectra of free and intracted drug were compared at different concentration of Cip (6.5×10^{-8} mol L^{-1}, Fig. 3a and 2.0×10^{-7} mol L^{-1}, Fig. 3b). The variation of AgNPs concentration was the same in both the cases, as determined by fluorescence spectroscopy. Free Cip has a broad emission peak around 430 nm, when excited at 335 nm (curve a). The curves b–f in Fig. 3b, c correspond to the adsorbed species on AgNPs. The adsorbed species has an emission spectrum centered at 410 nm and does interfere with the plasmonic absorption band of AgNPs (Fig. 3c). The observed blue shift in the emission and enhancing of the intensity can be attributed to the electronic interactions between the drug molecule and the AgNPs.

Figure 4 presents the effect of AgNPs concentration on the fluorescence intensity of Cip at the two different concentrations obtained by plotting the normalized fluorescence intensity at 410 nm as a function of AgNPs concentration. An enhancement or quenching of the fluorescence can be observed depending on the exact conditions. As can be seen, the fluorescence intensity increases, with increasing AgNPs concentration, up to about 6.0×10^{-6} mol L^{-1}, due to the interaction of drug with metal nanoparticle. However, for both of the Cip concentrations a decrease in fluorescence intensity was observed when AgNPs concentration increased up to 3.0×10^{-5} mol L^{-1}. This is most probably due to an increased collision probability between complex and free metal nanoparticles.

The quenching of fluorescence is known to occur by excited state reactions, complex formation (static quenching), energy transfer, and collisional quenching (dynamic quenching) [40]. The last two processes are mainly considered. When a donor molecule is placed in the vicinity of the conductive metal surface, resonant energy transfer between the donor and acceptor takes place [41]. The probability of Forster energy transfer depends on the

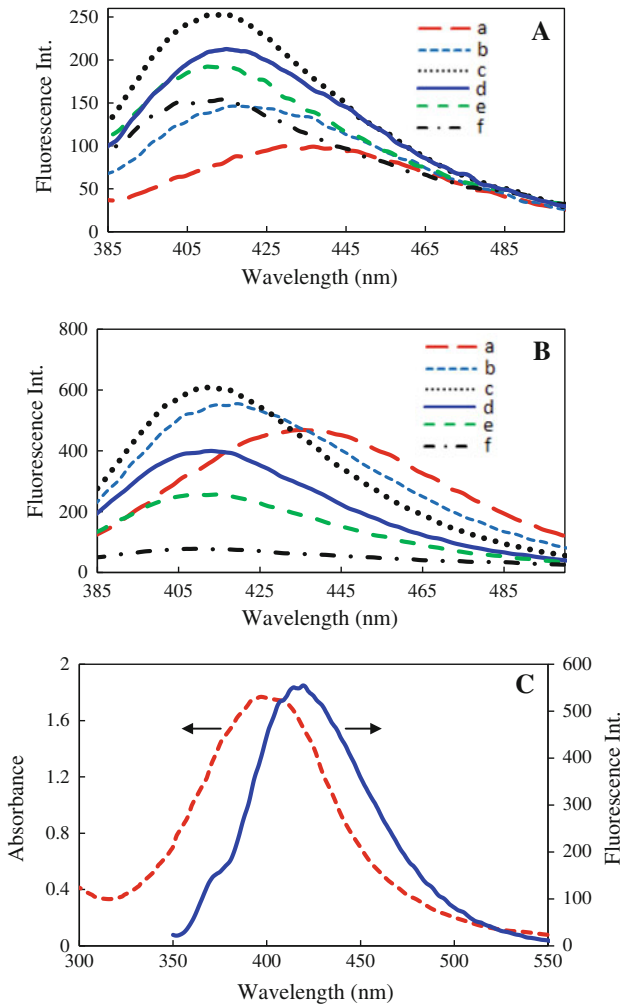

Fig. 3 Fluorescence emission spectra of different concentrations of Cip: **a** 6.5×10^{-8} mol L^{-1}, **b** 2.0×10^{-7} mol L^{-1} after addition of increasing amount of AgNPs to Cip, i.e., *a* 0, *b* 2.0×10^{-6}, *c* 6.0×10^{-6}, *d* 9.0×10^{-6}, *e* 2.0×10^{-5} and *f* 3.5×10^{-5} mol L^{-1}. **c** The overlap of the absorption spectrum of AgNPs, 5.0×10^{-5} mol L^{-1} (*left*) and emission spectrum of AgNPs-Cip, 2.0×10^{-7} mol L^{-1} (*right*)

overlap of the emission band of the probe molecules with the absorption spectrum of the nanoparticles. The energy transfer processes is considered to be the major deactivation pathways for excited Cip on the metal surface, resulting from the spectra interfere of Cip-AgNP with the plasmonic absorption band of AgNPs increasing. In the present case, there is a overlap of the emission band of Cip-AgNP and the absorption spectrum of the free AgNPs, which leads to the presence of Forster energy transfer between Cip-AgNP and excess free AgNPs (Fig. 3c).

On the other hand probably due to an increased concentration of AgNPs in solution, dynamic quenching occurs between bounded and free AgNPs. Dynamic, i.e., collisional quenching occurs when excited state fluorophore is deactivated upon contact with the quencher molecule in solution. In this case, the fluorophore is returned to the ground state during a diffusive encounter with the quencher.

The Stern–Volmer equation [30] accounting for quenching is written as Eq. (2):

$$I_0/I = 1 + K_{sv}[\text{AgNPs}] \quad (2)$$

where K_{sv} is quenching constant, I_0 and I are the fluorescence intensity of probe molecule in the absence and presence of quencher [AgNPs], respectively. The collisional quenching is effectively possible at the concentrations AgNPs $> 6 \times 10^{-6}$ mol L^{-1}. Figure 5 shows the plot of I_0/I versus [AgNPs] for two constant concentration of Cip. The plots are linear with $K_{sv} = 2.4 \times 10^4$ L mol^{-1}. The linearity of the Stern–Volmer plot indicates that only one type of quenching occurs in the system.

Dynamic quenching can be distinguished by their differing dependence on temperature. Higher temperature results in faster diffusion and larger amounts of collisional quenching. Figure 6 shows the effect of temperature change on the Stern–Volmer plots. As can be seen K_{sv} increased with increasing temperature (Table 1). This indicates that collisional quenching by dynamic

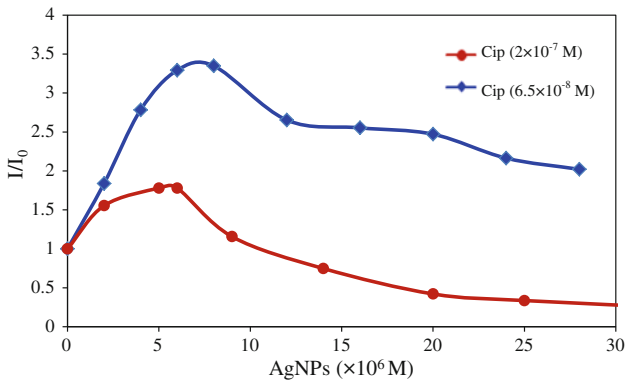

Fig. 4 Normalized fluorescence intensity variation (410 nm) of Cip versus AgNPs at two different concentrations of drug

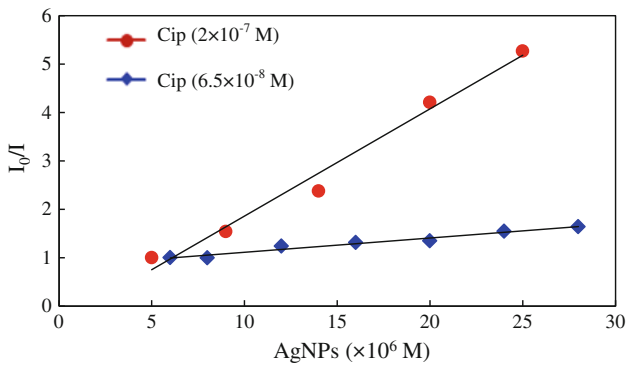

Fig. 5 Stern–Volmer curves for quenching effects of AgNPs on Cip fluorescence at two different concentration of drug

Table 1 Stern–Volmer quenching constants of the Cip-AgNPs

T (K)	K_{sv} (L mol^{-1})	R^2	k_q (L mol^{-1} s^{-1})	K_{as} (L mol^{-1})	E (kJ mol^{-1})
298	2.59×10^4	0.99	2.59×10^{12}	1.70×10^6	31.1
303	2.98×10^4	0.92	2.98×10^{12}		
310	4.09×10^4	0.96	4.09×10^{12}		
318	5.61×10^4	0.98	5.61×10^{12}		

mechanism does occur at [AgNPs] $> 6.0 \times 10^{-6}$ mol L^{-1}. According to bimolecular quenching, Eq. (3):

$$K_{sv} = k_q \times \tau_0 \quad (3)$$

where k_q is bimolecular rate constant and τ_0 (10^{-8} s) is the average lifetime of the fluorescence substance without quencher [40]. Therefore, according to Eq. (3), k_q were calculated as shown in Table 1. When the dynamic quenching mechanism is dominant, a plot of lnk_q versus inverse temperature gives an Arrhenius plot (Eq. 4):

$$\ln k_q = \ln A - E_a/RT \quad (4)$$

Values of E_a and the frequency factor A were derived from linear least squares regression plot of lnk_q versus 1/T. Plotting lnk_q versus 1/T yields excellent correlation coefficient ($R^2 = 0.99$) which is shown in Fig. 6. The slope directly provides the activation energy (E_a) of the collisional quenching of Cip-AgNPs in the presence of excess free AgNPs, which was found to be equal to 31.1 kJ mol^{-1}. In conclusion, dynamic quenching and energy transfer process is competing with each other.

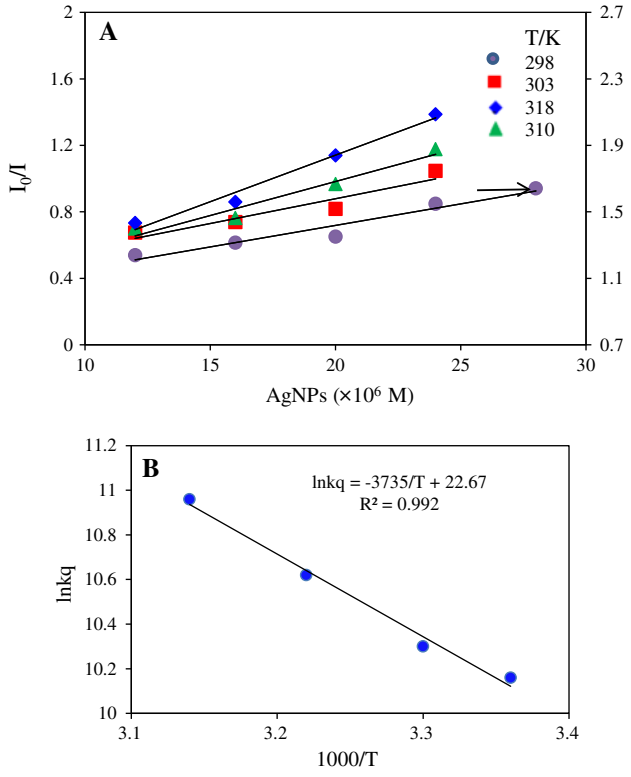

Fig. 6 Stern–Volmer plots for quenching effects of AgNPs on Cip fluorescence at different temperatures (**a**) and Arrhenius plots of lnk_q versus 1/T for dynamic quenching mechanism (**b**)

Analytical characteristics and application

To determining the linearity behavior of proposed method, a series of standard solutions of Cip in the concentration ranges of 1.0×10^{-7}–5.0×10^{-5} mol L^{-1} were examined under the optimum conditions (containing 6.0×10^{-6} mol L^{-1} AgNPs). The external calibration graph for the calculation of figures of merit of system is used according to the procedure described above. The linear range of the calibration curve is 5.0×10^{-7}–3.0×10^{-5} mol L^{-1}. The limit of detection (LOD) was given by the equation LOD $= 3 \times \sigma_b/S$, where σ_b is the standard deviation of the blank measurements ($n = 5$) and S is the slope of the calibration graph. The detection limit found was 2.0×10^{-8} mol L^{-1}. The relative standard deviation (RSD%) was about 2.3 % for five replicate.

Under the experimental condition, the proposed method was applied to the determination of Cip in tablet. Accuracy of the procedure is checked by the "added-found" method. The standard addition method was used in the determination of Cip content in tablet samples. The recovery% of the added pure drug was calculated as, recovery% $= [(C_t - C_a)/C_a] \times 100$, where C_t is the total drug concentration measured after standard addition and C_a is the drug concentration added to formulation.

Good recoveries ranging from 95 to 102 were attained for these determination with satisfactory analytical precisions (RSD < 2.5 %). The results are summarized in Table 2.

Conclusion

Optical absorption and fluorescence emission techniques have been employed to study the photo physical properties of Cip on AgNPs. The Cip molecules were adsorbed on the surface of the AgNPs, which leads to metal enhancing of fluorescence. The enhanced intensity of this system is strongly dependent on the AgNPs concentration. When the concentration of AgNPs is less than 6.0×10^{-6} mol L^{-1},

Table 2 Results of recovery assays to check the accuracy of the proposed method for tablet samples ($n = 5$)

Samples[a]	Added[b] ($\times 10^{-3}$ mol L^{-1})	Found ($\times 10^{-3}$ mol L^{-1})	Recovery (%)	RSD (%)
1	0	29.0	96–102[a]	2.2
2	7.8	36.8	95–102	2.4
3	19.5	48.5	96–102	2.3
4	46.8	75.8	97–101	2.2
5	53.3	82.3	95–102	1.9

[a] Ciprofloxacin 500 mg tablets

[b] Amounts before dilution

[c] Recovery % = $((C_t - C_f)/C_f) \times 100$, C_t and C_f are measured and formulation concentration of drug in tablet, respectively

the enhanced fluorescence intensity of this system is the largest. The process of fluorescence quenching of Cip-AgNPs by excess AgNPs indicate that the collisional quenching occurs and the quenching depends on the concentration of excess AgNPs.

Acknowledgments The financial support of the Research Council of Tarbiat Modares University and the Iranian Nanotechnology Initiative Office (INSF) are gratefully acknowledged.

References

1. G.A. Ozin, Adv. Mater. **4**, 612 (1992)
2. U. Kreibig, M. Vollmer, *Optical Properties of Metal Clusters* (Springer, Berlin, 1995), p. 78
3. M.A. Noginov, M. Vondrova, S.M. Williams, M. Bahoura, V.I. Gavrilenko, S.M. Black, V.P. Drachev, V.M. Shalaev, A. Sykes, J. Opt. A: Pure Appl. Opt. **7**, S219 (2005)
4. T. Uwada, R. Toyota, H. Masuhara, T. Asahi, J. Phys. Chem. C **111**, 1549 (2007)
5. C. Wang, M. Luconi, A. Masi, L. Fernández, in: D.P. Perez (Ed.), *Silver Nanoparticles as Optical Sensors, Silver Nanoparticles* (InTech, Vukovar, 2010), pp. 225–256
6. M. Umadevi, P. Vanelle, T. Terme, Beulah J.M. Rajkumar, V. Ramakrishnan, J Fluoresc. **19**, 3 (2009)
7. H. Lin, T. Ohta, A. Paul, J.A. Hutchison, K. Demid, O. Lebedev, G.V. Tendeloo, J. Hofkens, H. Uji, J. Photochem. Photobiol., A **221**, 220 (2011)
8. C.A. Sabatini, R.V. Pereira, M.H J Fluoresc. **17**, 377 (2007)
9. V.S. Lebedev, A.G. Vitukhnovsky, A. Yoshida, N. Kometani, Y. Yonezawa, Colloids Surf. A **326**, 204 (2008)
10. M. Singh, I. Sinha, A.K. Singh, R.K. Mandal, Colloids Surf. A **384**, 668 (2011)
11. N.L. Rosi, C.A. Mirkin, Chem. Rev. **105**, 1547 (2005)
12. P. Alivisatos, Nat. Biotechnol. **22**, 47 (2004)
13. T. Liu, D. Li, D. Yang, M. Jiang, Colloids Surf. A **387**, 17 (2011)
14. H. Xie, A.G. Tkachenko, W.R. Glomm, J.A. Ryan, M.K. Brennaman, J.M. Papanikolas, S. Franzen, D.L. Feldheim, Anal. Chem. **75**, 5797 (2003)
15. J.H. Liao, Y. Zhang, W. Yu, Colloids Surf. A **223**, 177 (2003)
16. A. Ivanisevic, C.A. Mirkin, J. Am. Chem. Soc. **123**, 7887 (2001)
17. H. Imahori, H. Norieda, H. Yamada, Y. Nishimura, I. Yamazaki, Y. Sakata, S. Fukuzumi, J. Am. Chem. Soc. **123**, 100 (2001)
18. X. Fang, H. Song, L. Xie, Q. Liu, H. Zhang, X. Bai, B. Dong, Y. Wang, W. Han, J. Chem. Phys. **131**, 54506 (2009)
19. A. Moadhen, H. Elhouichet, L. Nosova, M. Oueslati, J. Lumin. **126**, 789 (2007)
20. N. Chandrasekharan, P.V. Kamat, J. Hu, G. Jones II, J. Phys. Chem. B. **104**, 11103 (2000)
21. C. Lin, M.T. Berry, P. May, J. Lumin. **130**, 1907 (2010)
22. H.W. Sun, L.Q. Li, X.Y. Chen, Anal. Bioanal. Chem. **384**, 1314 (2006)
23. L.C. Jackson, L.A. Machado, M.L. Hamilton, Acta Med. **8**, 13 (1998)
24. D. Currie, L. Lynas, D.G. Kennedy, W.J. McCaughey, Food Addit. Contam. **15**, 651 (1997)
25. N. Lian, H.C. Zhai, C.Y. Sun, S.L. Chen, Y. Lu, L.P. Jin, Microchem. J. **74**, 223 (2003)
26. M. Bordbar, M. Shamsipur, N. Alizadeh, J. Photochem. Photobiol., A **178**, 83 (2006)
27. M. Aghamohammadi, J. Hashemi, G. Asadi, N. Alizadeh, Anal. Chim. Acta **582**, 288 (2007)
28. M. Aghamohammadi, N. Alizadeh, J. Lumin. **127**, 575 (2007)
29. J. Hashemi, G. Asadi, N. Alizadeh, Talanta, **75**, 1075 (2008)
30. J. Hashemi, N. Alizadeh, Spectrochim. Acta Part A. **73**, 121 (2009)
31. J.A. Creighton, C.G. Blathford, M.G. Albrecht, J. Chem. Soc. Faraday II **75**, 790 (1979)
32. J.R. Lakowicz, *Principles of fluorescence spectroscopy*, 2nd edn. (Kluwer Academic/Plenum Press, New York, 1999), pp. 280–290
33. H. Benesi, J.H. Hildebrand, J. Am. Chem. Soc. **71**, 2703 (1949)
34. Z. Wang, G. Chumanov, Adv. Mater. **15**, 1285 (2003)
35. T.R. Jensen, M.D. Malinsky, C.L. Haynes, R.P. Van Duyne, J. Phys. Chem. B **104**, 10549 (2000)
36. J.J. Mock, M. Barbic, D.R. Smith, D.A. Schultz, S. Schultz, J. Chem. Phys. **116**, 6755 (2002)
37. L. Rahman, R. Qureshi, M.M. Yasinzai, A. Shah, C. R. Chim. **15**, 533 (2012)
38. D. Pavia, G. Lampman, G. Kriz, *Introduction to spectroscopy*, 3rd edn. (Thomson Learning, Toronto, 2001), pp. 15–104
39. M. Zupancic, I. Arcon, P. Bukovec, A. Kodre, Croat. Chem. Acta **75**, 1 (2002)
40. P. Manikandan, V. Ramakrishnan, J. Fluoresc. **21**, 693 (2011)
41. C.T. Kenner, K.W. Busch, *In quantitative analysis* (Macmillan, New York, 1979), pp. 320–375